Available online at www.sciencedirect.com
ScienceDirect
Journal of the European Ceramic Society 28 (2008) 555–562
www.elsevier.com/locate/jeurceramsoc

Induced crystallization porosity and properties of sintereds diopside and wollastonite glass-ceramics

Alexander Karamanov [a,*], Mario Pelino [b]

[a] *Institute of Physical Chemistry, Bulgarian Academy of Sciences, G. Bonchev Str. Block 11, 1113 Sofia, Bulgaria*
[b] *Department of Chemistry, Chemical Engineering and Materials, University of L'Aquila, 67040 Monteluco di Roio-L'Aquila, Italy*

Accepted 1 August 2007
Available online 17 September 2007

Abstract

A diopside ($CaO{\cdot}MgO{\cdot}2SiO_2$) and wollastonite ($CaO{\cdot}SiO_2$) glass-ceramics, forming ~60% crystal phase and ~40% albite-like ($Na_2O{\cdot}Al_2O_3{\cdot}6SiO_2$) residual glass were studied. Two other diopside glass-ceramics with higher Na_2O and Al_2O_3 content were also investigated.

The phase formation was estimated by DTA, XRD and pycnometry, while the densification process was evaluated by porosity variations, dilatometry and SEM observations. The bending strength, Young modulus and coefficient of thermal expansion of the glass-ceramics were also measured and discussed.

The compositions were characterized by a good sinter-ability and surface crystallization and, due to the different volume variation of diopside and wollastonite during the crystallization, diverse amounts of intragranular *crystallization induced porosity*, P_{CR}, were formed in the glass-ceramics.

Notwithstanding the higher porosity, the diopside glass-ceramics have better mechanical properties than wollastonite one. At the same time, despite of the different residual glass compositions and the diverse coefficients of thermal expansion, all diopside materials have comparable bending strength and Young modulus.

The obtained diopside sintered glass-ceramics are characterized by significant porosity of 10–12 vol.%, high amount of residual glass (about 40%), large initial particles (<75 μm) and elevate crystal size (15–25 μm). Nevertheless high bending strength of 130 MPa and Young modulus of 100 GPa were obtained after only 1 min sinter-crystallization at 900 °C. The good mechanical properties were related to the P_{CR} formation.

Keywords: Glass-ceramics; Crystallization; Porosity; Mechanical properties; Sintering

1. Introduction

From a thermodynamic point of view the stable crystal phase has lower free energy and higher density than the corresponding unstable amorphous phase with the same composition.[1–4] For this reason the crystallization processes, related to the glass-ceramics production, are accompanied by a crystallization volume variation, ΔV_{CR}. Since the glass density is an additive function of the chemical composition,[3,5,6] while the density of crystal phases depends on their structure and packing [1,7] ΔV_{CR} varies significantly [4,8,9]: its value is lower at more loosely crystal structure and is higher at more dense arrangement.

The glass-ceramics are considered as non-porous materials [10–12] (i.e. it is assumed that the crystallization volume variation leads only to some shrinkage of the products and to increasing of the density). The occurrence of micro-voids, observed in some glass-ceramic samples, are explained as defects of the parent glasses or cracks, formed due to different coefficients of thermal expansion of the presented crystal and amorphous phases.[10–12] Similarly to the ceramic materials, the porosity is considered as a negative factor, which significantly reduces the mechanical properties. For this reason it is assumed that the absence of porosity in the glass-ceramic materials is one of their main advantages.

Another peculiarity of the crystallization process, related to glass-ceramics manufacturing, is the increase of apparent viscosity, η_a, due to phase formation. This phenomenon is well known in the glass-ceramics, produced by bulk nucleation and crystal growth, since it avoids their deformation during the heat-treatment.[10–12]

* Corresponding author. Tel.: +359 2 979 2552; fax: +359 2 971 2688.
E-mail address: karama@ipc.bas.bg (A. Karamanov).

0955-2219/$ – see front matter © 2007 Elsevier Ltd. All rights reserved.
doi:10.1016/j.jeurceramsoc.2007.08.001

In order to limit the deformation it is recommended to apply low heating rate between the nucleation and crystallization steps and to carry out the phase formation process always at η_a values superior than 10 dPa s.[10,11] It is also supposed that at high heating rate the stresses, formed by ΔV_{CR}, may create cracks in the sample, while at low heating rate the induced crystallization stresses are compensated by the slow viscous flow of residual glassy phase.

The variation of apparent viscosity also influences the synthesis of sintered glass-ceramics.[13] When the rate of phase formation is low, the sintering kinetics may be explained by the theories of viscous flow sintering,[14–17] while, when densification and crystallization take place simultaneously, the increasing of apparent viscosity may reduce the sintering rate and may inhibit the densification.[18–25]

Various models are proposed to explain the relationship between the apparent viscosity of a suspension and the corresponding volume of rigid phase.[26–28] Nevertheless of the differences in the theoretical approaches, all relations predict a relatively small variation up to one "critical" percentage of rigid phase, followed by rapid increasing of η_a by $10^{3–6}$ dPa s. In the case of sinter-crystallization this means that full densification can be obtained only if the sintering process completes before the formation of the "critical" percentage of crystalline phase; otherwise it will be inhibited by high apparent viscosity.

The densification of some sintered glass-ceramics is hindered after the formation of 5–15% of crystal phase [23,24] and the subsequent phase formation does not lead to any additional volume variations.[19–21,24,25] It follows that the increasing of η_a not only inhibits the sintering process but also hinders the shrinkage due to ΔV_{CR}. It can be concluded that only a part of the crystallization volume variation increases the apparent density, while the another part can be transformed into additional pores or/and can create tensile stresses in the material.

The formation of this porosity was noted by some authors,[29–32] but it was highlighted in details in our previous works,[33–35] where the crystallization volume variations, the kinetics of sinter-crystallizations and the properties of three compositions with albite ($Na_2O{\cdot}Al_2O_3{\cdot}6SiO_2$)–diopside ($CaO{\cdot}MgO{\cdot}2SiO_2$) compositions were discussed. The formed diopside is a phase with a high ΔV_{CR}, which leads to formation of intragranular spherical pores, named *induced crystallization porosity*, P_{CR}. The amount of the induced porosity increases as a function of the crystallization trend: about 60, 50 and 30 wt% diopside were formed in the three glass-ceramics, whereas the P_{CR} amount was estimated as about 8, 5 and 1 vol.%, respectively. Nevertheless of the increasing of porosity the mechanical properties improve with the rise of the crystallinity.

In the present work three new glasses were studied. In the first composition β-wollastonite ($CaO{\cdot}SiO_2$) (i.e. crystal phase with similar chain silicate structure as diopside but with a minimum ΔV_{CR} variation [8,9]) and albite residual glass are formed. In other two compositions the crystal phase remains diopside, but the residual albite glass is modified, becoming richer of Na_2O and Al_2O_3, respectively. The results were compared with the corresponding diopside–albite glass-ceramic.

2. Experimental

Glass batches were prepared by mixing quartz sand ($SiO_2 > 99.5\%$) with technically pure $Al(OH)_3$, $CaCO_3$, $MgCO_3$ and Na_2CO_3. The theoretical glass compositions (labelled W, D, D-Na and D-Al) are reported in Table 1, together with the values, obtained by XRF analysis (Spectro XEPOS) after glass melting. Both results are in a good agreement, except for the alumina content due to the corrosion of the crucibles.

The melting of glasses was carried out in 500 ml corundum crucibles for 2 h. D and W were melted at 1500 °C, while D-Na and D-Al at 1450 and 1550 °C, respectively. The melts were fritted and the obtained frits (about 250 g for each glass) were broken, milled and sieved. The milling was carried out in agate mill at 300 turns/min using portions of 50–60 g frit and milling time of 20 min.

The crystallization was evaluated by DTA (Linseiz L81) at 10 °C/min using powder (75–125 μm) and little bulk samples of about 100 mg.

"Green" samples with initial sizes 7/10/10 and 4/4/8 mm^3 were prepared by mixing fractions 75–125 μm with 7.5% PVA solution and by pressing at 100 MPa. The samples ware used to study the sintering by pycnometry and dilatometry, respectively.

After drying and a 30 min heat-treatment at 270 °C (to eliminate the PVA), the samples (7/10/10 mm^3) were held for 1 h at different temperatures, using heating and cooling rates of 20 °C/min. The densification was evaluated by measuring apparent, ρ_a, skeleton, ρ_s, and absolute, ρ_{gc}, densities and by estimation of corresponding total, P_T, closed, P_C, and open, P_O, porosities:

$$P_T = 100\frac{\rho_{gc} - \rho_a}{\rho_{gc}} \quad (1)$$

$$P_C = 100\frac{\rho_{gc} - \rho_S}{\rho_{gc}} \quad (2)$$

$$P_O = P_T - P_C \quad (3)$$

ρ_a was measured by a dry flow pycnometer (GeoPyc 1360), while ρ_s and ρ_{gc}—by He displacement Pycnometer (AccuPyc 1330). First the skeleton density was measured and then the absolute density after crashing and milling the samples below 26 μm. The experimental associated errors to the evaluation of ρ_a, ρ_{gc} and ρ_s were estimated as ±0.013, ±0.003 and ±0.005 g/cm^3, respectively, which correspond to ±0.6 and ±0.3% errors of P_T and P_C, respectively.

Table 1
Chemical compositions of studied glasses (t, theoretical and a, analysis results)

	D		D-Al		D-Na		W	
	t	a	t	a	t	a	t	a
SiO_2	54	53.0	54	53.5	54	53.2	54	51.9
Al_2O_3	2	2.1	4	5.2	–	0.7	2	4.6
CaO	21	22.1	21	19.6	21	22.6	42	41.6
MgO	21	20.6	21	17.9	21	19.6	–	–
Na_2O	2	2.2	–	–	4	3.9	2	1.9

The sintering was also studied by differential dilatometer (Netzsch 402 ED) at 10 °C/min employing 4/4/8 mm^3 samples. Detailed description of the used experimental technique is given in a previous work.[35]

The structure and morphology of the obtained glass-ceramics were investigated by a scanning electron microscopy (Philips XL30CP), after polishing and etching the surface for 3 or 10 s with 2 wt% HF solution, and by back scattering electrons (BSE) observation.

Phase analysis of the glass-ceramics was made by X-ray diffraction (Philips PW1830) with Cu Kα radiation. The amount of crystalline phase was estimated by comparing the amorphous and crystalline areas in the XRD spectra.

Crystalline fraction, x (wt%), was also evaluated by the density measurements through the following expression [9]:

$$x = 100\frac{1/\rho_g - 1/\rho_{gc}}{1/\rho_{g(cr)} - 1/\rho_{cr}} \quad (4)$$

ρ_g is the absolute density of the parent glass, ρ_{gc} the absolute density of the glass-ceramic, $\rho_{g(cr)}$ the density of a hypothetical glass with composition of the formed crystal phase and ρ_{cr} is the density of the crystal phase. The applicability of this method depends by the density difference between the crystal and corresponding amorphous structures (i.e. by ΔV_{CR}) and by the accuracy of density measurements. The experimental associated error to the measurements of ρ_g and ρ_{gc} was evaluated as ±0.003 g/cm^3. In case of diopside ρ_{cr} and $\rho_{g(cr)}$ have values of 3.27 and 2.75 g/cm^3, respectively, which corresponds to an error of ±1% crystal phase. In the case of wollastonite, ρ_{cr} and $\rho_{g(cr)}$ have similar values (2.92 and 2.87 g/cm^3, respectively), yielding an error of ±11% crystal phase.

3/4/50 mm^3 "green" samples were prepared by using the <75 μm glass fraction and pressing at 150 MPa. The samples were heated at 20 °C/min, held at the proper temperature range for sinter-crystallization and cooled at 5°/min. Series of five samples were used to evaluate the mechanical properties. The Young modulus was measured by means of the non-destructive resonance frequency technique (Grindosonic) and the bending strength was evaluated by a three point bending test with 40 mm outer span and a speed of 0.1 mm/min (SINTEC D/10).

The linear thermal expansion coefficients, CTE (20–400 °C) of the final glass-ceramics were evaluated at 5 °C/min by a Differential Dilatometer (Netzsch 402 ED).

3. Results and discussion

3.1. D and W glass-ceramics

Fig. 1 shows DTA traces of D and W powder and bulk samples. Both compositions present surface crystallization as demonstrated by the shift of the crystallization peak from bulk to powder samples. Crystallization peaks of the powder samples occur at 130–140 °C lower temperatures and have considerably higher intensity than the ones of bulk samples. The temperature differences between crystallization peak, T_p, and glass transition, T_g, temperatures are also comparable. Due to its inferior viscosity diopside composition has lower T_g and T_p.

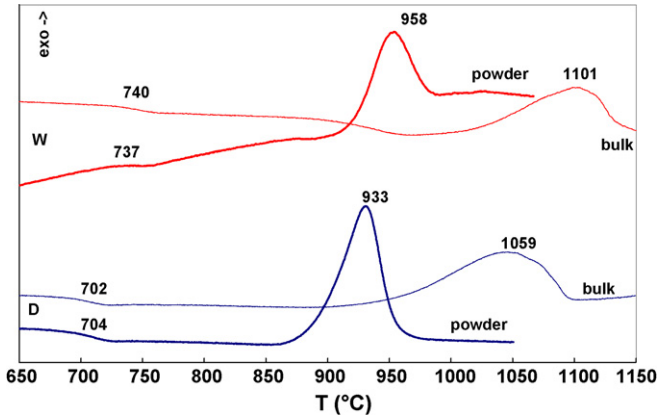

Fig. 1. DTA traces of powder and bulk D and W samples.

Fig. 2 presents the corresponding sintering curves and highlights that the densification in both compositions starts in the glass transition range and completes before the beginning of intensive phase formation (i.e. the sintering is not significantly influenced by the crystallization). The temperature shift between both dilatometric traces is similar to one, observed in the DTA results.

Apparent, absolute and skeleton densities, as a function of holding temperature, are shown in Figs. 3 and 4; the corresponding values of open, closed and total porosities are summarised in Figs. 5 and 6.

The variation of the apparent densities is similar for both glasses. In D and W, a remarkable increasing of ρ_{ap} is observed at 50–70 °C higher temperatures than the glass transition range (i.e. at 750 and 800 °C, respectively). The densification completes at 800 and 850 °C, respectively, and at higher temperatures the apparent densities remain constant.

The variation of skeleton density highlights the formation of closed porosity: when ρ_{sc} is equal to ρ_{as} the porosity is only open, while when ρ_{sc} is equal to ρ_{ap} the porosity is only closed. In W the porosity is mainly open up to 800 °C and then the microstructure evolves to closed porosity. In D, the porosity is open up to 750 °C, at 800 °C starts formation of closed porosity and at higher temperature the porosity is practically only closed.

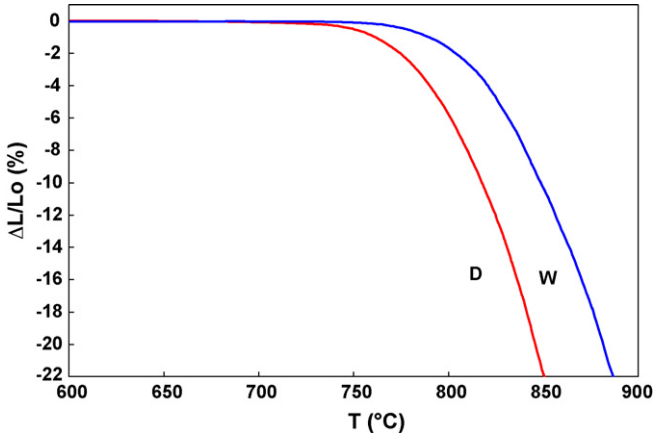

Fig. 2. Dilatometric sintering curves of D and W samples.

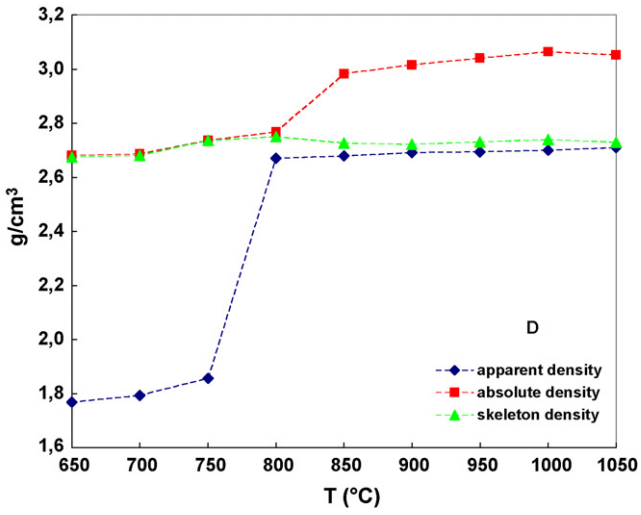

Fig. 3. Apparent, skeleton and absolute density of D composition vs. temperature.

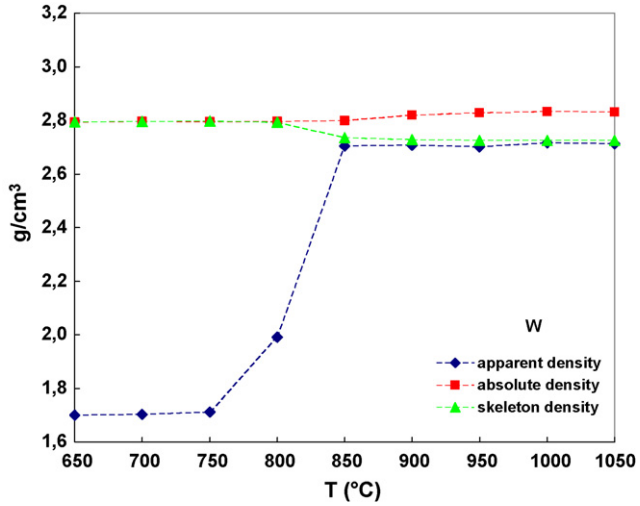

Fig. 4. Apparent, skeleton and absolute density of W composition vs. temperature.

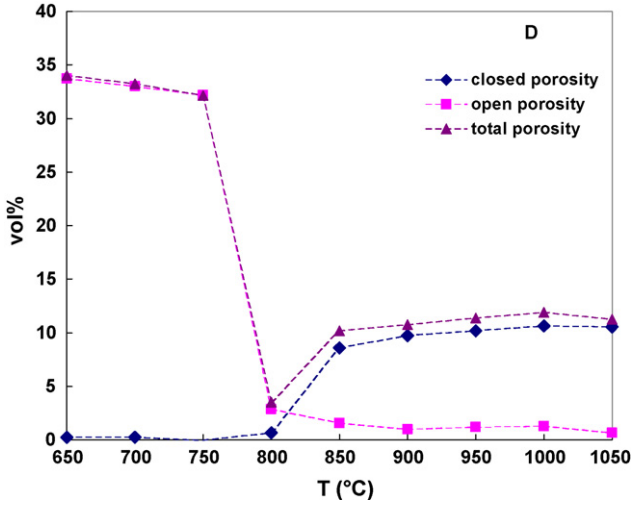

Fig. 5. Open, closed and total porosity of D composition vs. temperature.

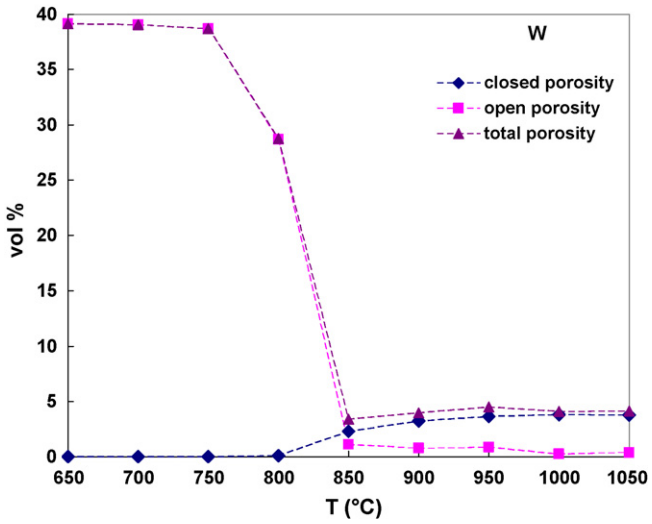

Fig. 6. Open, closed and total porosity of W composition vs. temperature.

The variation of absolute density is related to the phase formation. In diopside composition, which is characterized by a significant crystallization volume variation, ρ_{as} starts to increase at 750 and at 850–900 °C its value rises by 11–13%. In the wollastonite composition, where ΔV_{CR} is small, the absolute density increases by 1–1.5% in the phase formation range of 900–1050 °C.

Due to diverse crystallization volume variations both glass-ceramics are characterized by different closed porosity: in wollastonite composition (950–1050 °C) P_C is 4–4.5%, while in diopside glass-ceramic (900–1050 °C) it is 10–12%. Assuming that 3–4% of the porosity is intergranular residual porosity, P_{RE}, [1,2,15,17,30] it may be concluded that about 8% *induced crystallization porosity*, P_{CR}, is formed in D and about 1% in W.

SEM observations, shown in Figs. 7 and 8, confirm the elevate porosity in D and the more dense structure of W glass-ceramics, respectively.

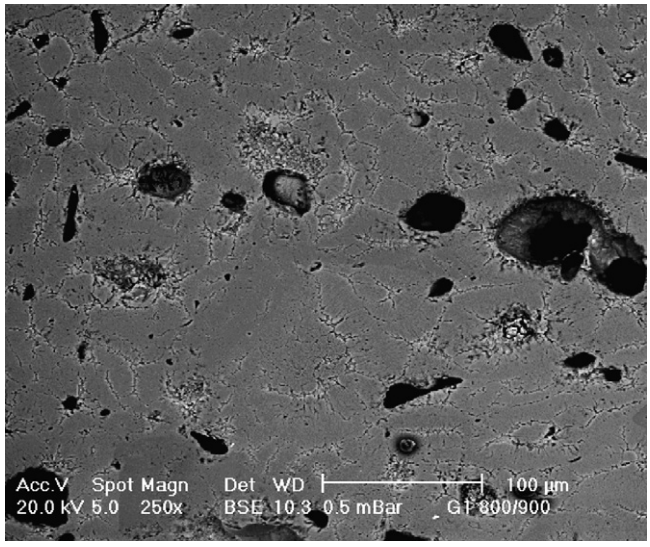

Fig. 7. BSE-SEM images of D glass-ceramic after 3 s etching time.

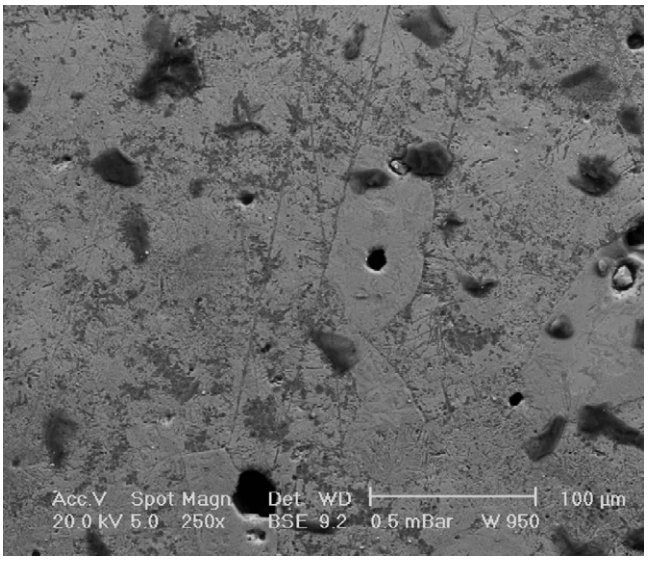

Fig. 8. BSE-SEM images of W glass-ceramic after 3 s etching time.

Fig. 9 presents BSE-SEM images at different magnifications of the diopside material. The two types of closed porosity are well distinguished: the intergranular residual pores have irregular shape and are characterized by a smooth surface, while intragranular-induced crystallization pores have semi-spherical shape and an indented polycrystalline surface.

The diameters of the crystallization pores are about 40–45% of the size of corresponding particles, which means that the pore volume is between 7 and 9% of the whole grain volume. This value is in a good agreement with the total P_{CR} amount and highlights that the formation of crystallization-induced pore takes place practically in each grain.

The structure of both kinds of pores at a 4000 magnification is presented in Fig. 10. Fig. 10a shows the smooth surface of a residual pore, where the beginning of surface crystallization is well distinguished; Fig. 10b presents the surface of an induced crystallization pore with the final part of the crystals growth, completing in the void, formed in the particle center.

Table 2
Properties of studied glass-ceramics

	Bending strength (MPa)	Young modulus (GPa)	Linear thermal expansion ($\times 10^{-7}$ deg^{-1})
D	132 ± 14	108 ± 3	88
D-Na	131 ± 13	105 ± 6	91
D-Al	137 ± 11	107 ± 5	77
W	76 ± 8	99 ± 2	65

In W glass-ceramic two kinds of porosity were also observed. The main part of the pores are residual intergranular voids, formed at the end of densification process and characterized by 20–70 μm sizes. Few new spherical intragranular pores with smaller size of 5–15 μm were also observed in the end of crystallization. Fig. 11a shows a typical residual pore with a smooth surface, formed after 1 h at 850 °C, while Fig. 11b is an image of the additional intragranular porosity, obtained at 950 °C.

The XRD spectra of D and W glass-ceramics obtained after 1 h at 900 and 950 °C, respectively, show comparable crystallinity values of 59 ± 4% diopside in D and 56 ± 4% β-wollastonite in W.

The coefficients of thermal expansion, CTE, of the glass-ceramics (Table 2) were compared with CTE values of formed crystal phases and hypothetical residual glasses. For diopside and β-wollastonite the data, obtained by Richet et al. [36] were used, while CTE of the residual glasses were estimated by Appen method.[5] The chemical compositions of residual glasses were evaluated as a function of parent glass compositions and the amounts of crystal phase formed.

In W glass-ceramic the measured coefficient of linear thermal expansion (65×10^{-7} K^{-1}) is similar to the β-wollastonite (63×10^{-7} K^{-1}) and lower than the residual glass ($73 \pm 3 \times 10^{-7}$ K^{-1}). At the same time, D glass-ceramic has a thermal expansion of 88×10^{-7} K^{-1}, while the diopside and the residual glass have lower values of 84×10^{-7} and $75 \pm 2 \times 10^{-7}$ K^{-1}, respectively. The unusually high CTE of D glass-ceramic may be explained by the dendritic colonnar

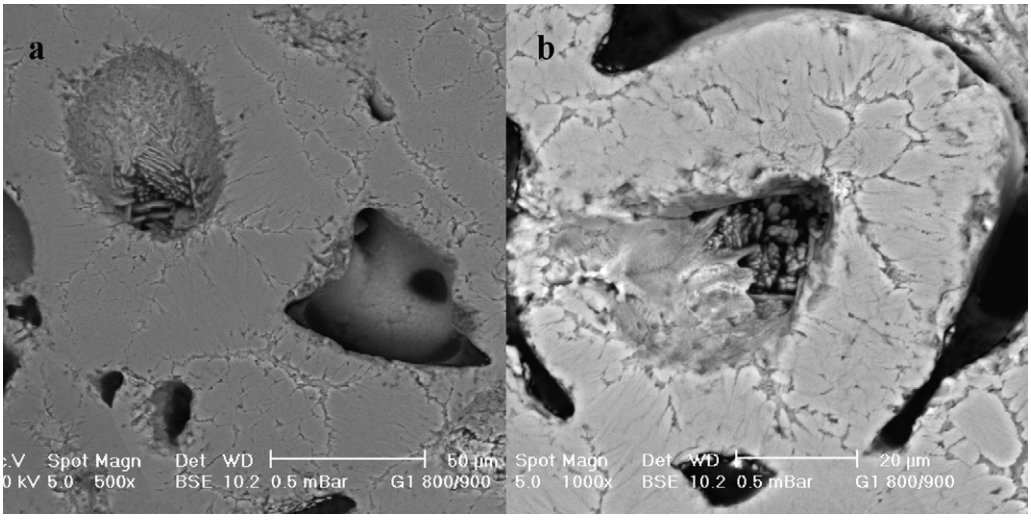

Fig. 9. BSE-SEM images of D glass-ceramic structure after 3 s etching time.

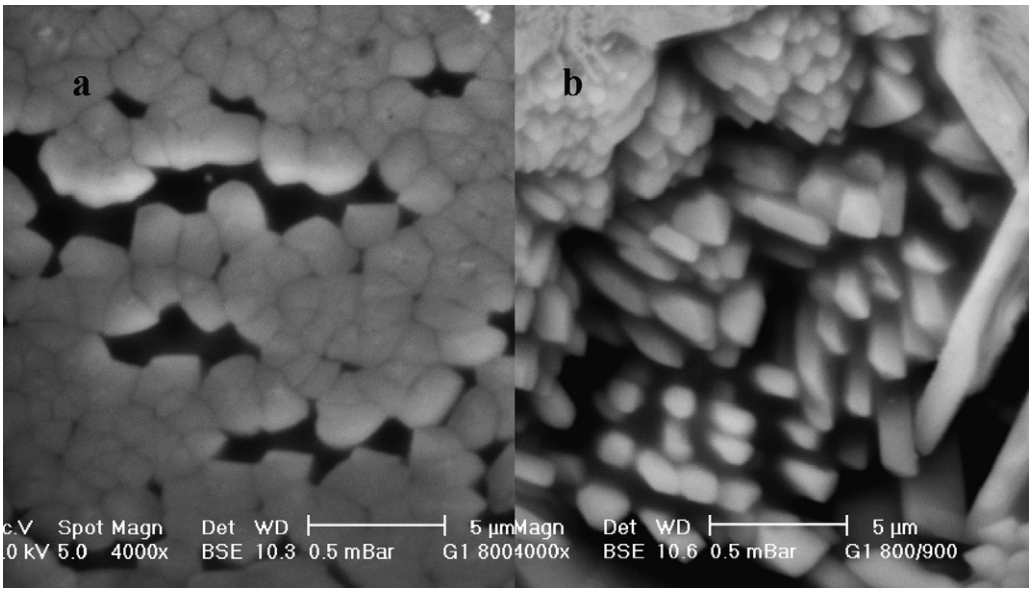

Fig. 10. BSE-SEM images of surface of residual pore (a) and crystallization-induced pore (b) in D glass-ceramic after 10 s etching time.

shape of the crystals[35] and by anisotropy of thermal expansion of diopside[36]: in the 20–400 °C range this phase has high CTE of $169.8 \times 10^{-7}\ K^{-1}$ in *b* crystallographic axis and low CTE of 55.2×10^{-7} and $56.3 \times 10^{-7}\ K^{-1}$ in *a* and *c* axes, respectively.

By the dilatometric results follows that tensile stresses can be formed in W residual glass (the amorphous phase has higher CTE than the glass-ceramic) and compressive stresses can be formed in D residual glass (the amorphous phase has lower CTE than the glass-ceramic).[10,11]

Table 2 also reports the bending strength and the Young modulus of D and W glass-ceramic samples. Notwithstanding of its higher porosity, D shows better properties than W, in apparent contradiction with the "traditional" knowledge about the mechanical properties of ceramic materials, which predict a significant decrease of the mechanical properties as function of the porosity.[1,2,27]

Since the two glass-ceramics have ∼40% albite-like residual glasses and similar surface crystallization behaviour two hypotheses might be proposed to explain the higher mechanical properties of D samples.

The first approach is based on the different CTE of the glass-ceramics. The traditional models, used to explain the mechanical properties of ceramic and glass-ceramic materials, assume that the characteristics improve at crystal phase with higher CTE than the residual glassy phase and decrease at crystal phase with lower CTE. It might be supposed that the positive effect due to the formation of reinforcing compressive stresses in the residual D glassy phase overcomes the negative effect caused by its higher porosity.

The second hypothesis considers that the formation of a high amount of *induced porosity* in D composition can significantly reduce the *crystallization stresses*. If the P_{CR} formation is neg-

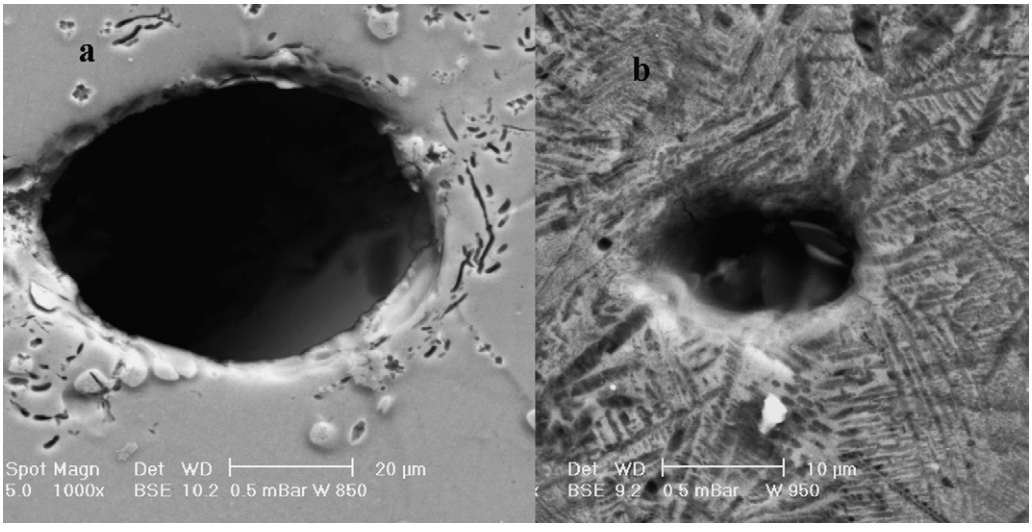

Fig. 11. BSE-SEM images of W glass-ceramic structure after 3 s etching time.

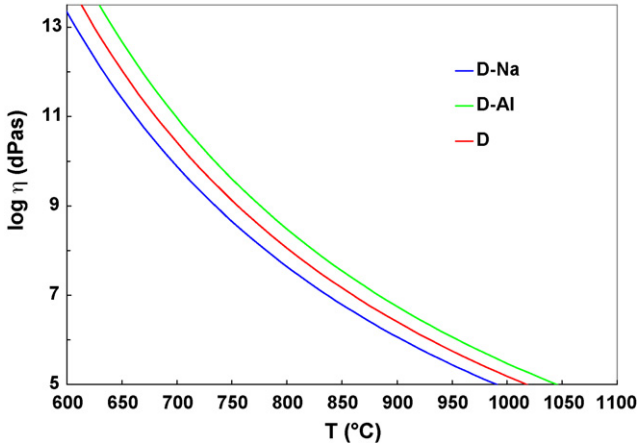

Fig. 12. Viscosity–temperature curves of diopside compositions, estimated by the Lakatos method.

ligible it may be assumed that a part of ΔV_{CR} variation can be transformed in internal tensile stresses, which will decrease the mechanical properties. Moreover, the formation of spherical pores in the centers of the grains might interrupt the propagation of micro-cracks.

In order to clarify the obtained result two other diopside composition were defined and investigated.

3.2. D, D-Na and D-Al glass-ceramics

The new diopside glasses contain equal percentages SiO_2, CaO and MgO as D composition and different amounts Na_2O and Al_2O_3. In D-Na the 2 mol% Al_2O_3 was substituted by Na_2O, whereas in D-Al the 2 mol% Na_2O was replaced with Al_2O_3. As a result, the viscosity in D-Na decreases and the coefficients of thermal expansion of parent and residual glasses increases, while in D-Al the viscosity increases and CTE decreases.

Hypothetical viscosity–temperature curves of the three diopside compositions, estimated by the Lakatos method,[3] are plotted in Fig. 12, while Figs. 13 and 14 show D-Na, D and D-Al dilatometric and DTA results, respectively.

The densification plots of the three diopside compositions highlight that the sintering starts in the glass transition range and completes before the beginning of crystallization; the temperature shifts of the sintering curves are similar to the viscosity variations. The DTA traces demonstrate that the T_g and T_P changes also are in agreement with the expected viscosity differences.

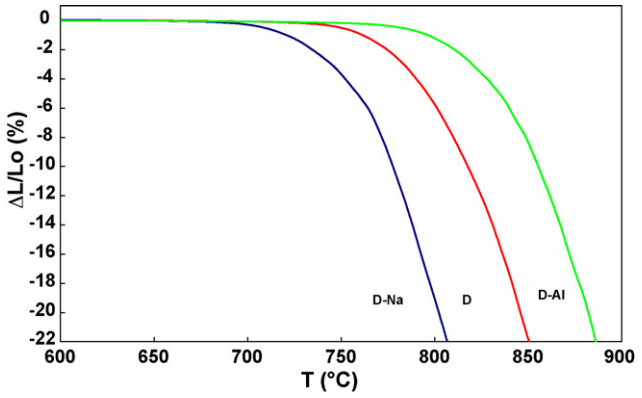

Fig. 13. Dilatometric sintering curves of D, D-Na and D-Al samples.

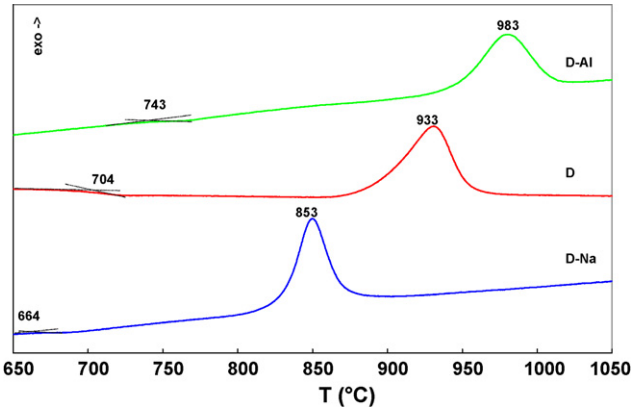

Fig. 14. DTA traces of powder D, D-Na and D-Al samples.

At the same time the DTA exo-therms become broader and with lower intensity in order D-Na, D and D-Al. This feature may be related to the different variations of residual glass compositions during the phase formation. The residual melt in D-Na becomes richer of Na_2O, which decreases the viscosity and increases the crystallization rate, while in D-Al the viscosity increases, reducing the velocity of phase formation and increasing the crystallization time; in D a negligible viscosity variation is expected during the phase formation.[33]

D-Na and D-Al samples were heat-treated at different temperatures for different times and the degrees of sintering and crystallization were evaluated by pycnometry measurements. About 64 and 58 wt% diopside and 9–10 and 8–9 vol.% P_C were measured in D-Na and D-Al glass-ceramics, respectively, by complete sinter-crystallization obtained after 1 min at 900 °C for D-Na and 60 min at 950 °C for D-Al.

The three diopside glass-ceramics have comparable porosities and percentages of formed crystal phase, but, due to different chemical compositions of the residual glasses, are characterized by diverse coefficients of thermal expansion (Table 2).

CTE of the residual glasses, estimated by Appen method,[5] corresponds to $95 \pm 2 \times 10^{-7}\,K^{-1}$ for D-Na (i.e. higher value than the glass-ceramic) and $41 \pm 2 \times 10^{-7}\,K^{-1}$ for D-Al (i.e. lower value than the glass-ceramic), respectively. It follows that compressive stresses might be formed in D-Al glassy phase and tensile stresses in one of D-Na.[10,11] It might be assumed that improvement of the mechanical properties can be expected in D-Al glass-ceramic and decreasing in D-Na. Moreover, due to high Na_2O and low Al_2O_3 percentages, D-Na residual glass must have the lowest mechanical resistance.

The Young modulus and bending strength of the three diopside compositions however are comparable, which highlights that the mechanical characteristics in the studied glass-ceramics mainly depend on the formation of *crystallization induced porosity* and their specific structures. The new diopside glass-ceramics are characterized by large initial particles, elevate crystal length of 15–25 μm, about 40% residual glass and about

10% porosity. Nevertheless, their mechanical properties are comparable to the fine-crystalline bulk glass-ceramics,[10–12] produced by long two step thermal treatment, and to the advanced ceramics materials, obtained by sintering of fine powders at high temperatures.[1,2,27]

The relationship between the P_{CR} formation and the relaxation of the *induced crystallization stresses* in glass-ceramics, as well as the kinetics of formation of nano- and micro-*crystallization induced porosity*, will be the objects of future investigations.

4. Conclusions

The structure and properties of a diopside and a wollastonite-sintered glass-ceramics, forming ~60% crystal phase and ~40% albite-like residual glasses, are compared. Both compositions are characterized by good sinter-ability and surface crystallization but, due to the crystallization volume variation of diopside and wollastonite, different intragranular *crystallization induced porosity*, P_{CR}, are formed. The diopside glass-ceramic is characterized by higher with about 8 vol.% porosity but with a 70% superior bending strength.

Two other diopside compositions with higher Na_2O and Al_2O_3, contents, forming similar amount of crystal phase and P_{CR}, were also investigated. The glass-ceramics are characterized by different residual glasses and coefficients of thermal expansion but have similar mechanical properties.

Bending strength of 130 MPa and Young modulus of 100 GPa were obtained after only 1 min heat-treatment at 900 °C.

References

1. Kingery, W. D., Bowen, H. K. and Uhlmann, D. R., *Introduction to Ceramics*. John Willey & Sons, New York, 1975.
2. Hlavac, J., *The Technology of Glass and Ceramics: an Introduction*. Elsevier, Amsterdam, 1983.
3. Scholze, H., *Glass Nature, Structure and Properties*. Springer-Verlag, Berlin, 1990.
4. Gutzow, I. and Shmelzer, J., *The Vitreous State-Structure, Thermodynamics, Rheology and Crystallisation*. Springer-Verlag, Berlin, 1995.
5. Appen, A. A., *The Chemistry of Glasses*. Himiq, Leningrad, 1974 [in Russian].
6. Volf, M. B., *Chemical Approach to Glasses*. Elsevier, Amsterdam, 1984.
7. Liebau, F., *Structural Chemistry of Silicates*. Springer-Verlag, Berlin, 1985.
8. Zanotto, E. D. and Muler, E. A., A simple method to predict the nucleation mechanism in glass. *J. Non-Cryst. Solids*, 1991, **130**, 220–221 [Letter to the Editor].
9. Karamanov, A. and Pelino, M., Evaluation of the degree of crystallisation in glass-ceramics by density measurements. *J. Eur. Ceram. Soc.*, 1999, **19**(5), 649–654.
10. McMillan, P. W., *Glass-Ceramics*. Academic Press Inc., London, 1979.
11. Strnad, Z., *Glass-Ceramic Materials*. Elsevier, Amsterdam, 1986.
12. Höland, W. and Beall, G., *Glass-Ceramics Technology*. The American Ceramics Society, Westerville, 2002.
13. Gutzow, I., Paskova, R., Karamanov, A. and Schmelzer, J., The kinetics of surface induced sinter-crystallization and the formation of glass-ceramic materials. *J. Mater. Sci.*, 1998, **33**(21), 5265–5273.
14. Frenkel, J., Viscous flow of crystalline bodies under the action of surface tension. *J. Phys. USSR*, 1945, **9**(5), 385–391.
15. Mackenzie, J. K. and Shuttleworth, R., A phenomenological theory of sintering. *Proc. Phys. Soc. (London), Sec. B*, 1949, **62**, 833.
16. Scherer, G. W., Sintering of low-density glasses. I. Theory. *J. Am. Ceram. Soc.*, 1977, **60**(5–6), 236–241.
17. Prado, M. O., Zanotto, E. D. and Müller, R., Model for sintering polydispersed glass particles. *J. Non-Cryst. Solids*, 2001, **279**(2–3), 169–178.
18. Panda, P. and Ray, R., Sintering and Crystallization of glass at constant heating rate. *J. Am. Ceram. Soc.*, 1989, **72**(8), 1564–1566.
19. Müller, R., On the kinetics of sintering and crystallization of glass powders. *Glastech. Ber. Glass Sci. Technol.*, 1994, **67C**, 93–99.
20. Boccaccini, A. R., Stumpfe, W., Taplin, D. M. R. and Ponton, C. B., Densification and crystallization of glass powder compacts during constant heating rate sintering. *Mater. Sci. Eng. A*, 1996, **219**, 26–31.
21. Winter, W., Sintering and crystallization of volume- and surface-modified cordierite glass powders. *J. Mater. Sci.*, 1997, **32**, 1649–1655.
22. Sujirote, K., Rawlings, R. D. and Rogers, P. S., Effect of fluoride on sinterability of a silicate glass powder. *J. Eur. Ceram. Soc.*, 1998, **18**, 1325–1330.
23. Karamanov, A., Pelino, M. and Hreglich, A., Sintered glass-ceramics from MSW-incinerator fly ashes. Part I. The influence of the heating rate on the sinter-crystallisation. *J. Eur. Ceram. Soc.*, 2003, **23**, 827–832.
24. Aloisi, M., Karamanov, A. and Pelino, M., The sintering behaviour of MSWI ash glass. *J. Non-Cryst. Solids*, 2004, **345–346**, 192–196.
25. Karamanov, A., Aloisi, M. and Pelino, M., Sintering behaviour of a glass obtained from MSWI ash. *J. Eur. Ceram. Soc.*, 2005, **25**, 1531–1540.
26. Krieger, I. M., Rheology of monodispersed latices. *Adv. Colloid Interf. Sci.*, 1972, **3**, 111–117.
27. Reed, J. S., *Principles of Ceramic Proceedings* (*2nd ed.*). John Wiley & Sons, New York, 1995.
28. Fan, Z. and Boccaccini, A. R., A new approach to the effective viscosity of suspension. *J. Mater. Sci.*, 1996, **31**, 2515–2521.
29. Ryu, B. and Yasui, I., Sintering and crystallization behavior of a glass powder and bloks with a composition of anorthite and the microstructure dependence of its thermal expansion. *J. Mater. Sci.*, 1994, **29**, 3323–3328.
30. Marghussian, V. K. and Dayi Niaki, M. H., Effects of composition changes on the crystallization behavior and properties of SiO_2–Al_2O_3–CaO–MgO (Fe_2O_3–Na_2O–K_2O) glass-ceramics. *J. Eur. Ceram. Soc.*, 1995, **15**, 343–348.
31. Pascual, M. J., Duran, A. and Pascual, L., Sintering process of glasses in the system Na_2O–B_2O_3–SiO_2. *J. Non-Cryst. Solids*, 2002, **306**, 58–69.
32. Tulyaganov, D. U., Agathopoulos, S., Ventura, J. M., Karakassides, M. A., Fabrichnaya, O. and Ferriera, J. M. F., Synthesis of glass–ceramics in the CaO–MgO–SiO_2 system with B_2O_3, P_2O_5, Na_2O and CaF_2 additives. *J. Eur. Ceram. Soc.*, 2006, **26**, 1463–1471.
33. Karamanov, A., Arrizza, L., Matecovetc, I. and Pelino, M., Properties of sintering glass-ceramics belonging to the system diopside–albite. *Ceram. Int.*, 2004, **30**, 2129–2135.
34. Karamanov, A. and Pelino, M., Sinter-crystallization in the system diopside–albite. Part I. Formation of induced crystallisation porosity. *J. Eur. Ceram. Soc.*, 2006, **26**, 2511–2517.
35. Karamanov, A. and Pelino, M., Sinter-crystallization in the system diopside–albite. Part II. Kinetics of crystallization and sintering. *J. Eur. Ceram. Soc.*, 2006, **26**, 2519–2526.
36. Richet, P., Mysen, B. O. and Ingrin, J., High-temperature X-ray diffraction and Raman spectroscopy of diopside and pseudowollastonite. *Phys. Chem. Mater.*, 1998, **25**, 401–414.